PHYSICAL REVIEW E **87**, 010901(R) (2013)

Spontaneous motion of an elliptic camphor particle

Hiroyuki Kitahata,[1,2,*] Keita Iida,[3] and Masaharu Nagayama[4,5]

[1]*Department of Physics, Graduate School of Science, Chiba University, Chiba 263-8522, Japan*
[2]*PRESTO, JST, Saitama 332-0012, Japan*
[3]*Graduate School of Natural Science and Technology, Kanazawa University, Kanazawa 920-1192, Japan*
[4]*Research Institute for Electronic Science, Hokkaido University, Sapporo 001-0020, Japan*
[5]*CREST, JST, Saitama 332-0012, Japan*

(Received 27 September 2012; published 7 January 2013)

The coupling between deformation and motion in a self-propelled system has attracted broader interest. In the present study, we consider an elliptic camphor particle for investigating the effect of particle shape on spontaneous motion. It is concluded that the symmetric spatial distribution of camphor molecules at the water surface becomes unstable first in the direction of a short axis, which induces the camphor disk motion in this direction. Experimental results also support the theoretical analysis. From the present results, we suggest that when an elliptic particle supplies surface-active molecules to the water surface, the particle can exhibit translational motion only in the short-axis direction.

DOI: 10.1103/PhysRevE.87.010901 PACS number(s): 82.40.Bj, 47.54.Fj, 47.63.mf, 68.03.Cd

Spontaneous motion in nonequilibrium systems has long attracted the interest of scientists because it is related to the motion of living organisms. In particular, the coupling between deformation and spontaneous motion has been actively investigated and several important and interesting studies, both experimental and theoretical, have been reported. For example, Ohta *et al.* proposed a generic model for the coupling between deformation and spontaneous motion by analyzing such coupling from the viewpoint of the bifurcation theory of dynamical systems [1–3]. Teramoto *et al.* studied the coupling between deformation and motion in pulse propagation in a reaction-diffusion system [4]. In experiments, cell motion is analyzed in relation to cell shape [5–7], and mathematical models have also been proposed for such cell deformation [8,9].

For investigating the coupling between motion and deformation, one approach is to decouple them; i.e., we consider the effect of particle shape on motion. For this purpose, we chose a camphor-water system, in which a camphor particle exhibits spontaneous motion but not deformation. The camphor-water system was first reported in the 19th century [10,11]. As a camphor particle is placed on pure water, it exhibits spontaneous motion. The mechanism of the motion is briefly described as follows [12,13]: Camphor molecules escape from the camphor particle to the water surface. Since camphor has a surface activity, the camphor molecules at the water surface reduce the surface tension. It should be noted that the camphor molecules sublimate to the air, so that the profile of the surface concentration of camphor molecules at the water surface can reach a steady state. If the camphor particle is circular and does not move, the profile of the surface concentration of camphor molecules should be symmetric with respect to the center of the camphor particle. However, it is known that such a steady state can become unstable by an infinitesimal fluctuation. In such a case, motion in a certain direction at a constant velocity is stabilized and realized. Consequently, the profile of the surface concentration becomes asymmetric [14–16]. This camphor-water system has attracted attention since it exhibits interesting and complicated phenomena such as collective motion [17–19] and jamming [20] in spite of its simple setup.

Using this camphor-water system, we investigate the effect of particle shape on the motion. To describe the particle shape, we consider small deformation from a circle with a radius R as a perturbation. In two-dimensional polar coordinates r and θ, the shape can be written as

$$r(\theta) = R\left[1 + \sum_{k=2}^{\infty}(a_k \cos k\theta + b_k \sin k\theta)\right], \tag{1}$$

where a_k and b_k are infinitesimal parameters. It is noted that the one-mode terms drop out since they mean only translation within the first order of the infinitesimal parameters. Thus, in the present Rapid Communication, we consider the two-mode deformation, which is the most fundamental but nontrivial deformation, corresponding to the deformation to an elliptic shape. To investigate the translational motion of an elliptic camphor particle, we use perturbation theory. We also perform experiments to support the results obtained by the analysis. We note that the present analysis is done for the camphor-water system, but it can be easily adapted to other systems in which surface tension is the driving force of the droplet, such as a water-alcohol system [21], or an aniline droplet [22].

The model equation is derived based on previous works [14,15,23]. First, we describe the shape of the camphor particle. By taking the symmetric properties into consideration, we only consider motion in the x direction, and the shape is written as

$$r(\theta) = R(1 + \epsilon \cos 2\theta), \tag{2}$$

by dropping the sine term, where ϵ is an infinitesimally small parameter for the deformation. It is noted that the long axis is in the x-axis direction as ϵ is positive and the short axis is in the x-axis direction as ϵ is negative. In other words, we can analyze the motion in the long- and short-axis directions by considering the x-axis-directed motion with positive ϵ and negative ϵ, respectively.

*Corresponding author: kitahata@physics.s.chiba-u.ac.jp

We consider a two-dimensional plane corresponding to the water surface, on which the surface concentration of camphor molecules is defined as $u(x,y,t)$. Here, x and y are the coordinates in space and t denotes time. The time derivative of u is written as

$$\frac{\partial u}{\partial t} = D\nabla^2 u - \alpha u + f(x,y). \tag{3}$$

The first term on the right-hand side is the surface diffusion of the camphor molecules with diffusion constant D, the second term is the sublimation of the camphor molecules to the air with a rate of α, and the third term is the supply of the camphor molecules from the camphor particle, where $f(x,y)$ is described as

$$f(x,y) = \begin{cases} f_0, & \text{if} \quad (x,y) \in \Omega(\mathbf{r}_c), \\ 0, & \text{otherwise}. \end{cases} \tag{4}$$

Here, $\Omega(\mathbf{r}_c)$ is the region in two-dimensional space that corresponds to the shape of the camphor particle depending on the center of mass $\mathbf{r}_c$.

For the equation of motion of the camphor particle, we adopt

$$m\frac{d^2\mathbf{r}_c}{dt^2} = -\eta\frac{d\mathbf{r}_c}{dt} + \mathbf{F}, \tag{5}$$

where m is the mass, η is the friction constant of the camphor particle, and $\mathbf{F}$ is the force exerted on the camphor particle, which is calculated as

$$\mathbf{F} = \int_{\partial\Omega} \gamma \mathbf{e}_n \, d\ell, \tag{6}$$

where γ is the surface tension determined by the concentration of camphor molecules at each position, $\mathbf{e}_n$ is the outer unit normal vector of the camphor particle, and $d\ell$ is the line element of $\partial\Omega$. From experiments, it has been found that the surface tension is a decreasing function of the surface concentration of the camphor molecules [24], and we assume a linear relation between γ and u for simplicity:

$$\gamma = \gamma_0 - \kappa u, \tag{7}$$

where κ is a positive constant. It is noted that the hydrodynamic effect such as Marangoni convection may exist, but we neglect it for simplicity.

In the present study, we choose η in Eq. (5) as a control parameter, and the bifurcation point η_0 with respect to η is obtained using a perturbation method. It is noted that a larger η_0 means that a camphor particle is easier to move.

To obtain the bifurcation point, we consider the solution propagating at a constant velocity. By considering a co-moving frame at velocity v, $u(x,y,t) = u(x - vt, y)$, Eq. (3) becomes

$$-v\frac{\partial u}{\partial x} = D\nabla^2 u - \alpha u + f(x,y), \tag{8}$$

or

$$-v\left(\cos\theta\frac{\partial}{\partial r} - \frac{\sin\theta}{r}\frac{\partial}{\partial\theta}\right)u = D\left(\frac{\partial^2}{\partial r^2} + \frac{1}{r}\frac{\partial}{\partial r} + \frac{1}{r^2}\frac{\partial^2}{\partial\theta^2}\right)u - \alpha u + f(r,\theta), \tag{9}$$

in polar coordinates. We also adopt the boundary conditions $u \to 0$ as $r \to \infty$, $\partial u/\partial r \to 0$ as $r \to +0$ and $|u| < \infty$ as $r \to +0$. From the solvability condition, u should be a C^1-class function, which leads to the following continuity conditions:

$$u^{(\mathrm{i})}(R(1+\epsilon\cos 2\theta),\theta) = u^{(\mathrm{o})}(R(1+\epsilon\cos 2\theta),\theta), \tag{10}$$

$$\nabla u^{(\mathrm{i})}|_{r=R(1+\epsilon\cos 2\theta)} = \nabla u^{(\mathrm{o})}|_{r=R(1+\epsilon\cos 2\theta)}, \tag{11}$$

where $^{(\mathrm{i})}$ and $^{(\mathrm{o})}$ denote the regions inside and outside the camphor particle Ω, respectively.

We assume that v and ϵ are infinitesimally small, and u is expanded with respect to v and ϵ. Under these conditions, the concentration profiles $u^{(\mathrm{i})}$ and $u^{(\mathrm{o})}$ for the inside and the outside of the camphor particle, respectively, are written as

$$u^{(\mathrm{i})} = u_{00}^{(\mathrm{i})} + \epsilon u_{01}^{(\mathrm{i})} + v\left(u_{10}^{(\mathrm{i})} + \epsilon u_{11}^{(\mathrm{i})}\right) + O(\epsilon^2, v^2), \tag{12}$$

$$u^{(\mathrm{o})} = u_{00}^{(\mathrm{o})} + \epsilon u_{01}^{(\mathrm{o})} + v\left(u_{10}^{(\mathrm{o})} + \epsilon u_{11}^{(\mathrm{o})}\right) + O(\epsilon^2, v^2). \tag{13}$$

Then, Eq. (9) can be expanded with respect to v as

$$0 = D\left(\frac{\partial^2}{\partial r^2} + \frac{1}{r}\frac{\partial}{\partial r} + \frac{1}{r^2}\frac{\partial^2}{\partial\theta^2}\right)u_{0\beta}^{(s)} - au_{0\beta}^{(s)} + f(r,\theta), \tag{14}$$

$$-\left(\cos\theta\frac{\partial}{\partial r} - \frac{\sin\theta}{r}\frac{\partial}{\partial\theta}\right)u_{0\beta}^{(s)} = D\left(\frac{\partial^2}{\partial r^2} + \frac{1}{r}\frac{\partial}{\partial r} + \frac{1}{r^2}\frac{\partial^2}{\partial\theta^2}\right)u_{1\beta}^{(s)} - au_{1\beta}^{(s)}, \tag{15}$$

where $^{(s)}$ denotes $^{(\mathrm{i})}$ or $^{(\mathrm{o})}$, and β denotes 0 or 1.

The continuity conditions (10) and (11) can also be expanded with respect to ϵ, giving

$$u^{(\mathrm{i})} + \epsilon\frac{\partial u^{(\mathrm{i})}}{\partial r}R\cos 2\theta = u^{(\mathrm{o})} + \epsilon\frac{\partial u^{(\mathrm{o})}}{\partial r}R\cos 2\theta, \tag{16}$$

and

$$\frac{\partial u^{(\mathrm{i})}}{\partial r} + \epsilon\frac{\partial^2 u^{(\mathrm{i})}}{\partial r^2}R\cos 2\theta + 2\epsilon\frac{\sin 2\theta}{R}\frac{\partial u^{(\mathrm{i})}}{\partial\theta} = \frac{\partial u^{(\mathrm{o})}}{\partial r} + \epsilon\frac{\partial^2 u^{(\mathrm{o})}}{\partial r^2}R\cos 2\theta + 2\epsilon\frac{\sin 2\theta}{R}\frac{\partial u^{(\mathrm{o})}}{\partial\theta}, \tag{17}$$

at $r = R$.

Using these conditions, we can straightforwardly calculate

$$u_{00}^{(\mathrm{i})} = \frac{f_0}{\alpha}[1 - \rho\mathcal{K}_1(\rho)\mathcal{I}_0(\tilde{r})], \tag{18}$$

$$u_{00}^{(\mathrm{o})} = \frac{f_0}{\alpha}\rho\mathcal{I}_1(\rho)\mathcal{K}_0(\tilde{r}), \tag{19}$$

$$u_{01}^{(\mathrm{i})} = \frac{f_0}{\alpha}\rho^2\mathcal{K}_2(\rho)\mathcal{I}_2(\tilde{r})\cos 2\theta, \tag{20}$$

$$u_{01}^{(\mathrm{o})} = \frac{f_0}{\alpha}\rho^2\mathcal{I}_2(\rho)\mathcal{K}_2(\tilde{r})\cos 2\theta, \tag{21}$$

$$u_{10}^{(\mathrm{i})} = \frac{f_0}{2\sqrt{D\alpha^3}}[\rho\mathcal{K}_1(\rho)\mathcal{I}_0(\tilde{r})\tilde{r} - \rho^2\mathcal{K}_2(\rho)\mathcal{I}_1(\tilde{r})]\cos\theta, \tag{22}$$

$$u_{10}^{(\mathrm{o})} = -\frac{f_0}{2\sqrt{D\alpha^3}}[\rho\mathcal{I}_1(\rho)\mathcal{K}_0(\tilde{r})\tilde{r} - \rho^2\mathcal{I}_2(\rho)\mathcal{K}_1(\tilde{r})]\cos\theta, \tag{23}$$

$$u_{11}^{(\mathrm{i})} = \frac{f_0}{4\sqrt{D\alpha^3}}[\rho^3\mathcal{K}_1(\rho)\mathcal{I}_1(\tilde{r}) - \rho^2\mathcal{K}_2(\rho)\mathcal{I}_2(\tilde{r})\tilde{r}]\cos\theta - \frac{f_0}{4\sqrt{D\alpha^3}}[\rho^2\mathcal{K}_2(\rho)\mathcal{I}_2(\tilde{r})\tilde{r} - \rho^3\mathcal{K}_3(\rho)\mathcal{I}_3(\tilde{r})]\cos 3\theta, \tag{24}$$

$$u_{11}^{(\mathrm{o})} = \frac{f_0}{4\sqrt{D\alpha^3}}[\rho^3\mathcal{I}_1(\rho)\mathcal{K}_1(\tilde{r}) - \rho^2\mathcal{I}_2(\rho)\mathcal{K}_2(\tilde{r})\tilde{r}]\cos\theta - \frac{f_0}{4\sqrt{D\alpha^3}}[\rho^2\mathcal{I}_2(\rho)\mathcal{K}_2(\tilde{r})\tilde{r} - \rho^3\mathcal{I}_3(\rho)\mathcal{K}_3(\tilde{r})]\cos 3\theta, \tag{25}$$

where $\mathcal{I}_n$ and $\mathcal{K}_n$ are the modified Bessel functions of the nth order of the first and second kind, respectively, $\rho = R\sqrt{\alpha/D}$, and $\tilde{r} = r\sqrt{\alpha/D}$.

The force exerted on the camphor particle is thus calculated as

$$\mathbf{F} = (F_0 + \epsilon F_1)v\mathbf{e}_x + O(\epsilon^2, v^3), \tag{26}$$

where F_0 and F_1 are explicitly written as

$$F_0 = \frac{\pi\kappa f_0 R^4}{4D^2}[\mathcal{I}_0(\rho)\mathcal{K}_0(\rho) - \mathcal{I}_2(\rho)\mathcal{K}_2(\rho)], \tag{27}$$

$$F_1 = -\frac{\pi\kappa f_0 R^4}{2D^2}[\mathcal{I}_1(\rho)\mathcal{K}_1(\rho) - \mathcal{I}_2(\rho)\mathcal{K}_2(\rho)]. \tag{28}$$

The signs of F_0 and F_1 are positive and negative, respectively, considering $\mathcal{I}_n(x)\mathcal{K}_n(x) > \mathcal{I}_{n+1}(x)\mathcal{K}_{n+1}(x)$ for any $x > 0$ and for any non-negative integer n [25]. The equation of motion along the x axis becomes

$$m\frac{dv}{dt} = -\eta v + (F_0 + \epsilon F_1)\, v + O(\epsilon^2, v^3). \tag{29}$$

This equation means that the camphor particle can move in the x-axis direction when η is less than $F_0 + \epsilon F_1$. In other words, the friction constant at the bifurcation point, η_0, is equal to $F_0 + \epsilon F_1$. Considering that the x axis corresponds to the long- and short-axis direction when ϵ is positive and negative, respectively, and that F_1 is negative, η_0 for the long-axis-directed translational motion is smaller than that for the short-axis-directed one. This means that the elliptic camphor particle tends to move in the short-axis direction at least with small deformation and within the neighborhood of the bifurcation point.

We can successively expand the steady-state concentration profile to the order of v^3, and we can obtain the steady-state velocity v as

$$0 = -\eta v + (F_0 + \epsilon F_1)v + (G_0 + \epsilon G_1)v^3 + O(\epsilon^2, v^5), \tag{30}$$

where

$$G_0 = \frac{\pi\kappa f_0 R^6}{32D^4}\left[\mathcal{I}_0(\rho)\mathcal{K}_0(\rho) - \frac{2}{\rho^2}\mathcal{I}_1(\rho)\mathcal{K}_1(\rho) - \mathcal{I}_2(\rho)\mathcal{K}_2(\rho)\right], \tag{31}$$

$$G_1 = \frac{\pi\kappa f_0 R^6}{48D^4}[-3\mathcal{I}_0(\rho)\mathcal{K}_0(\rho) + 4\mathcal{I}_1(\rho)\mathcal{K}_1(\rho) - \mathcal{I}_2(\rho)\mathcal{K}_2(\rho)]. \tag{32}$$

Since G_0 is negative, we can show that the supercritical bifurcation occurs. We can also calculate the steady-state velocity near the bifurcation point as

$$v = \pm\sqrt{-\frac{F_0 + \epsilon F_1 - \eta}{G_0 + \epsilon G_1}}. \tag{33}$$

To confirm the analysis mentioned above, we performed experiments using a camphor-water system. We prepared an elliptic camphor particle by putting camphor powder (Wako, Japan) into a purchased ellipse template (No. E201N, Sanko, Japan). The long- and short-axis lengths and thickness of the elliptic camphor particle were ∼13.5, ∼6.5, and ∼1.0 mm, respectively. The upper surface of the camphor particle was colored with black ink for easier visualization. Then, the prepared camphor particle was placed onto 1 L pure water (Matsuba, Japan) in a rectangular container with a size of ∼320 mm by ∼230 mm, and thus the depth of the water was around 15 mm. The image was taken from above using a digital video camera (DR-XR520V, Sony, Japan). All the experiments were performed at room temperature. The obtained image was analyzed with image processing software (ImageJ, National Institutes of Health, USA).

Figure 1 shows the experimental results for the motion of an elliptic camphor particle. The superposed images shown in Fig. 1(a) and the plots of the direction of velocity against that of the short axis shown in Fig. 1(b) indicate that the elliptic camphor particle moves in the short-axis direction. These experimental results are consistent with the analysis using the perturbation method.

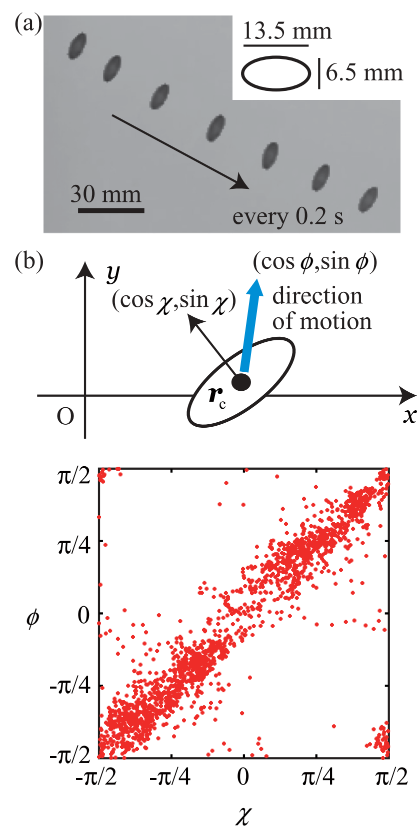

FIG. 1. (Color online) Experimental results of the spontaneous motion of an elliptic camphor particle. (a) Superposed images of an elliptic camphor particle every 0.2 s. The shape and size of the camphor particle are shown in the inset. See the movie in the Supplemental Material [26]. (b) Correlation between χ and ϕ during 60 s, where χ is the angle of the short-axis direction from the x axis, and ϕ is the angle of the direction of the velocity from the x axis. The plot points are concentrated along $\chi = \phi$, which means χ and ϕ are almost equal.

In the present Rapid Communication, we consider the steady-state solution in a co-moving frame and expand it with regard to v. As another approach, we can also expand the equation of motion using Green's function. By such a procedure, we can derive the normal form of the bifurcation [27]. The expansion for the shape or deformation is rather complicated for higher orders of ϵ. Instead, it seems to be possible using elliptic coordinates and Mathieu functions. These problems remain for future work.

From the present linear theory, important characteristics can be revealed. Here, we restrict the discussion to the spontaneous motion of a droplet or a particle driven by the surface tension gradient, which is caused by the chemicals supplied from the droplet or particle. In this case, the droplet or particle can exhibit spontaneous motion only when the chemical reduces the surface tension; in other words, $\kappa > 0$. Then, if the droplet or particle deforms in the form of an ellipse, it should move in the short-axis direction. This result suggests that the parameter a in Ohta and Ohkuma's paper [1] is positive for a self-propelled particle or droplet whose motion is originated from the surface tension gradient generated by the particle or droplet itself, where the parameter s in Ohta's model [1] corresponds to ϵ in this Rapid Communication, as long as $|s|$ is small.

We can make predictions about another case of spontaneous particle or droplet motion: In the case in which a particle or droplet consumes the chemicals supplied from the surroundings [28], the droplet can move only when the chemical increases the surface tension. Using a parallel discussion, we can show that the spontaneous motion occurs in the short-axis direction also in such a case.

In summary, we analyzed the spontaneous motion of an elliptic camphor particle using the perturbation method, and we showed that the friction constant at the bifurcation point is larger for the motion in the short-axis direction, which means that an elliptic camphor particle moves in the short-axis direction. In the experiments, the elliptic camphor particle was shown to move in the short-axis direction, which supports the theoretical result. Analysis for large deformation from the circular shape, that for rotational motion, and that with hydrodynamic effect remain for future studies.

The authors thank Professor T. Ohta (Kyoto University), Professor Y. Nishiura (Tohoku University), Professor H. Nishimori (Hiroshima University), and Professor S. Nakata (Hiroshima University) for helpful discussions.

[1] T. Ohta and T. Ohkuma, Phys. Rev. Lett. **102**, 154101 (2009).
[2] T. Hiraiwa, M. Y. Matsuo, T. Ohkuma, T. Ohta, and M. Sano, Europhys. Lett. **91**, 20001 (2010).
[3] T. Hiraiwa, K. Shitara, and T. Ohta, Soft Matter **7**, 3083 (2011).
[4] T. Teramoto, K. Suzuki, and Y. Nishiura, Phys. Rev. E **80**, 046208 (2009).
[5] K. Keren, Z. Pincus, G. M. Allen, E. L. Barnhart, G. Marriott, A. Mogilner, and J. A. Theriot, Nature (London) **453**, 475 (2008).
[6] Y. T. Maeda, J. Inose, M. Y. Matsuo, S. Iwaya, and M. Sano, PLoS ONE **3**, e3734 (2008).
[7] L. Bosgraaf and P. J. M. van Haastert, PLoS ONE **4**, e5253 (2009).
[8] D. Shao, W.-J. Rappel, and H. Levine, Phys. Rev. Lett. **105**, 108104 (2010).
[9] F. Ziebert, S. Swaminathan, and I. S. Aranson, J. R. Soc. Interface **9**, 1084 (2012).
[10] C. Tomlinson, Proc. R. Soc. London **11**, 575 (1860).
[11] L. Rayleigh, Proc. R. Soc. London **47**, 364 (1890).
[12] S. Nakata, Y. Iguchi, S. Ose, M. Kuboyama, T. Ishii, and K. Yoshikawa, Langmuir **13**, 4454 (1997).
[13] Y. Hayashima, M. Nagayama, and S. Nakata, J. Phys. Chem. B **105**, 5353 (2001).
[14] A. S. Mikhailov and V. Calenbuhr, *From Cells to Societies* (Springer, Berlin, 2002).
[15] M. Nagayama, S. Nakata, Y. Doi, and Y. Hayashima, Physica D **194**, 151 (2004).
[16] X. Chen, S.-I.- Ei, and M. Mimura, Networks Hetrog. Media **4**, 1 (2009).
[17] S. Soh, K. J. M. Bishop, and B. A. Grzybowski, J. Phys. Chem. B **112**, 10848 (2008).
[18] S. Soh, M. Branicki, and B. A. Grzybowski, J. Phys. Chem. Lett. **2**, 770 (2011).
[19] E. Heisler, N. J. Suematsu, A. Awazu, and H. Nishimori, J. Phys. Soc. Jpn. **81**, 074605 (2012).
[20] E. Heisler, N. J. Suematsu, A. Awazu, and H. Nishimori, Phys. Rev. E **85**, 055201 (2012).
[21] K. Nagai, Y. Sumino, H. Kitahata, and K. Yoshikawa, Phys. Rev. E **71**, 065301 (2005).
[22] Y.-J. Chen, Y. Nagamine, and K. Yoshikawa, Phys. Rev. E **80**, 016303 (2009).
[23] H. Kitahata and K. Yoshikawa, Physica D **205**, 283 (2005).
[24] Y. S. Ikura, R. Tenno, H. Kitahata, N. J. Suematsu, and S. Nakata, J. Phys. Chem. B **116**, 992 (2012).
[25] Á. Baricz and S. Ponnusamy, Proc. Am. Math. Soc. **141**, 523 (2013).
[26] See Supplemental Material at http://link.aps.org/supplemental/10.1103/PhysRevE.87.010901 for the movie of the spontaneous motion of an elliptic camphor particle in an experiment.
[27] S. Yabunaka, T. Ohta, and N. Yoshinaga, J. Chem. Phys. **136**, 074904 (2012).
[28] Y. Sumino and K. Yoshikawa, Chaos **18**, 026106 (2008).